Hydrogen-Bond Interactions of the Primary Donor of the Photosynthetic Purple Sulfur Bacterium *Chromatium tepidum*†

Anabella Ivancich,*,‡ Masayuki Kobayashi,§ Friedel Drepper,|| Insan Fathir,§ Takayuki Saito,§ Tsunenori Nozawa,§ and Tony A. Mattioli‡

Section de Biophysique des Protéines et des Membranes and Section de Bioénergétique, Département de Biologie Cellulaire et Moléculaire, CEA and URA CNRS 1290, Centre d'Etudes de Saclay, 91191 Gif-sur-Yvette, cedex, France, and Department of Biochemistry and Engineering, Faculty of Engineering, Tohoku University, Aramaki, Aoba, Sendai 980-77, Japan

Received December 27, 1995; Revised Manuscript Received May 15, 1996⊗

ABSTRACT: We have used near-infrared Fourier transform (pre)resonance Raman spectroscopy to determine the protein interactions with the bacteriochlorophyll (BChl) dimer constituting the primary electron donor, P, in the reaction center (RC) from the thermophilic purple sulfur bacterium *Chromatium tepidum*. In addition, we report the alignment of partial sequences of the L and M protein subunits of *C. tepidum* RCs in the vicinity of the primary donor with those of *Rhodobacter sphaeroides* and *Rhodopseudomonas viridis*. Taken together, these results enable us to propose the hydrogen-bonding pattern and the H-bond donors to the conjugated carbonyl groups of P. Selective excitation (1064-nm laser radiation) of the FT (pre)-resonance Raman spectra of P in its neutral (P°) and oxidized ($P^{\bullet+}$) states were obtained via their electronic absorption bands at 876 and 1240 nm, respectively. The P° spectrum exhibits vibrational frequencies at 1608, 1616, 1633, and 1697 cm^{-1} which bleach upon P oxidation. The $P^{\bullet+}$ spectrum exhibits new bands at 1600, 1639, and 1719 cm^{-1}. The 1608-cm^{-1} band, which downshifts to 1600 cm^{-1} upon oxidation, is assigned to a C_aC_m methine bridge stretching mode of the P dimer, indicating that each BChl molecule possesses a single axial ligand (His L181 and His M201, from the sequence alignment). The 1616- and 1633-cm^{-1} bands correspond to two H-bonded π-conjugated acetyl carbonyl groups of each BChl molecule, with different H-bond strengths: the 1616-cm^{-1} band is assigned to the P_L C_2 acetyl group which is H-bonded to a histidine residue (His L176), while the 1633-cm^{-1} band is assigned to the P_M C_2 acetyl carbonyl, H-bonded to a tyrosine residue (Tyr M196). Both P_L and P_M C_9 keto carbonyls are free from interactions and vibrate at the same frequency (1697 cm^{-1}). Thus, the H-bond pattern of the primary donor of *C. tepidum* differs from that of *Rb. sphaeroides* in the extra H-bond to the P_M C_2 acetyl carbonyl group; that of P_L is H-bonded to a histidine residue in both primary donors (His L168 in *Rb. sphaeroides* and His L176 in *C. tepidum*). The $P^\circ/P^{\bullet+}$ redox midpoint potentials were measured to be +497 and +526 mV for isolated *C. tepidum* RCs with and without the associated tetraheme cytochrome *c* subunit, respectively, and +502 mV for intracytoplasmic membranes. The positive charge localization was estimated to be 69% in favor of P_L, indicating a more delocalized situation over the primary donor of *C. tepidum* than that of *Rb. sphaeroides* (estimated to be 80% on P_L). These differences in physicochemical properties are discussed with respect to the proposed structural model for the microenvironment of the primary donor of *C. tepidum*.

Chromatium tepidum is a thermophilic, photosynthetic purple sulfur bacterium taxonomically classified within the Chromatiaceae family, like the mesophilic sulfur bacterium *Chromatium vinosum* (Madigan, 1984, 1986); more specifically, Chromatiaceae belong to the γ subgroup of the Proteobacteria according to the 16S ribosomal RNA-based classification (Woese, 1987; Blankenship, 1992). *C. tepidum* grows autotrophically, oxidizing sulfide to elemental sulfur, which is stored within the cells (Madigan, 1984). The optimal temperature for growth is *ca.* 50 °C, which is 20 °C higher than for its mesophilic congener *C. vinosum* (Madigan, 1984) but 10 °C lower than the thermophilic green gliding bacterium *Chloroflexus aurantiacus*.

The photosynthetic apparatus of *C. tepidum* is comprised of bacteriochlorophyll (BChl)[1] *a*-containing proteins. Like in *C. vinosum*, two light-harvesting antenna complexes are present in the intracytoplasmic membranes of *C. tepidum*. One antenna complex possesses BChl *a* molecules absorbing at 800 and 855 nm (B800−850) while the other, although equivalent to the B890 antenna complex of *C. vinosum*, absorbs at 917 nm (Nozawa *et al*., 1986; Garcia *et al*., 1986). Both antenna complexes were reported to be stable up to 70 °C in isolated intracytoplasmic membranes (chromatophores); in contrast, when these complexes were isolated from their native lipid environment, only the B800−855 maintained

† A.I. gratefully acknowledges a postdoctoral fellowship from CONICET (Argentina). F.D. gratefully acknowledges a fellowship from the European Community.

* Corresponding author.

‡ Section de Biophysique des Protéines et des Membranes, Centre d'Etudes de Saclay.

§ Tohoku University.

|| Section de Bioénergétique, Centre d'Etudes de Saclay.

⊗ Abstract published in *Advance ACS Abstracts,* July 15, 1996.

[1] Abbreviations: RC(s), reaction center(s); BChl, bacteriochlorophyll; BPhe, bacteriopheophytin; P, primary electron donor; FT, Fourier transform; *Rps*., *Rhodopseudomonas*; *Rb*., *Rhodobacter*; *Rs*., *Rhodospirillum*; *Rvx*., *Rubrivivax*; *C*., *Chromatium*; *Cf*., *Chloroflexus*; OG, *n*-octyl β-D-glucopyranoside; Tris, tris(hydroxymethyl)aminomethane; FWHM, full width at half-maximum; NHE, normal hydrogen electrode.

S0006-2960(95)03047-9 CCC: $12.00

stability at high temperatures (Nozawa *et al*., 1986). The isolated B917 antenna complex irreversibly lost its characteristic absorption band above 50 °C, indicating that this complex is more thermostable when it is associated in chromatophores (Nozawa *et al*., 1986).

The isolated reaction center (RC) from *C. tepidum* (Nozawa *et al*., 1987; Garcia *et al*., 1987) consists of three polypeptide subunits, named L, M, and H, analogous to those found in *Rhodopseudomonas viridis* and *Rhodobacter sphaeroides*. In addition, it possesses a bound *c*-type tetraheme cytochrome containing two high-potential (*c*-556) and two low-potential (*c*-553) hemes (Nozawa *et al*., 1987). Both ubiquinones and menaquinones are present in whole cell extracts, but only a single active menaquinone is present in isolated RCs (Nozawa *et al*., 1987); this is consistent with the finding that in the *C. vinosum* RC Q_A is a menaquinone (Romijin & Amesz, 1977). Isolated RCs from *C. tepidum* show stability up to 45 °C as monitored by the electronic absorption band at 885 nm and circular dichroism spectrum, whereas those from thermophilic *Cf. aurantiacus* showed stability up to 60 °C (Nozawa & Madigan, 1991).

Reaction centers from photosynthetic purple bacteria have been the most extensively characterized to date, in particular those from the α subgroup (e.g., *Rb. sphaeroides*, *Rps. viridis*, *Rhodobacter capsulatus*). The three-dimensional crystal structure at atomic resolution has been solved for RCs from only two species of purple bacteria, *Rps. viridis* (Deisenhofer & Michel, 1989; Deisenhofer *et al*., 1995) and *Rb. sphaeroides* (Yeates *et al*., 1988; El-Kabbani *et al*., 1991; Chirino *et al*., 1994; Ermler *et al*., 1994). The X-ray crystallographic structures reveal that both reaction centers are composed of three polypeptide subunits, the L, M, and H subunits. In addition, the *Rps. viridis RC* possesses a fourth c-type tetraheme cytochrome subunit which is tightly bound. The common L, M, and H protein subunits noncovalently bind the following cofactors: two excitonically interacting bacteriochlorophyll (designated P_L and P_M) molecules which serve as the primary electron donor (P), two accessory BChl molecules ($BChl_L$ and $BChl_M$), two bacteriopheophytin molecules ($BPhe_L$ and $BPhe_M$), two quinones [menaquinone (Q_A) and ubiquinone (Q_B) for *Rps. viridis* and both ubiquinones for *Rb. sphaeroides*], a nonheme iron atom, and a carotenoid molecule. All these cofactors are arranged in pairs along a pseudo-C_2 symmetry axis which runs across the membrane resulting in two nearly symmetric branches associated with the L and M subunits, only the former appearing to be photochemically active.

Near-infrared Fourier transform (FT) Raman spectroscopy using 1064-nm excitation has been applied to determine the pigment−protein interactions in the primary donor of bacterial reaction centers, in particular those containing BChl *a* molecules (Mattioli *et al*., 1991, 1992a, 1993; Agalidis *et al*., 1992; Feiler *et al*., 1995; Goldsmith *et al*., 1996; Ivancich *et al*., 1996). The main advantage of this technique is the selectivity of the excitation wavelength used, since it enhances (i) the preresonance vibrational spectrum of the primary donor in its neutral ground state (P°) via its electronic absorption band at *ca*. 860 nm and (ii) the genuine resonance Raman vibrational spectrum of the oxidized primary donor ($P^{\bullet+}$) absorbing at *ca*. 1250 nm (Mattioli *et al*., 1991). In the *Rb. sphaeroides* RC, the C_2 acetyl carbonyl of the P_L constituent of P is engaged in a H-bond donated by His L168 (El-Kabbani et al., 1991; Ermler *et al*., 1994; Mattioli *et al*., 1991); breaking this H-bond results in a decrease of 95 mV in the $P°/P^{\bullet+}$ redox midpoint potential (Lin *et al*., 1994; Mattioli *et al*., 1995). Moreover, introduction of new single and multiple histidine-donated H-bonds to the conjugated carbonyl groups of P results in an increase of the $P°/P^{\bullet+}$ redox midpoint potential ranging from 60 to 260 mV (Lin *et al*., 1994; Mattioli *et al*., 1994, 1995). In contrast, the introduction of a H-bond donated by a Tyr residue on the P_M C_2 acetyl carbonyl group of the primary donor of *Rb. sphaeroides* RC induces a modest increase of *ca*. 25 mV in the redox potential (Wachtveitl *et al*., 1993). The primary donor of *Cf. aurantiacus* is observed to possess only one acetyl carbonyl engaged in a H-bond, the P_M C_2 acetyl carbonyl, probably donated by a Tyr residue (Ivancich *et al*., 1996) and the $P°/P^{\bullet+}$ redox midpoint potential is *ca*. 100 mV lower than that of *Rb. sphaeroides* (Bruce *et al*., 1982).

In this work, near infrared FT (pre)resonance Raman spectroscopy is used to determine the H-bond interactions of the *C. tepidum* primary donor with the protein and to deduce its microenvironmental structure. The H-bond pattern for the π-conjugated carbonyl groups of each BChl *a* molecule constituting the primary donor of *C. tepidum* RC is proposed by analogy to the FT Raman results on *Rb. sphaeroides* (wild type and mutants) RCs (Mattioli *et al*., 1991, 1994). Moreover, we report in this work the sequence alignment of the L and M subunits of *Rb. sphaeroides* and *Rps. viridis* for the amino acid residues in the vicinity of the primary donor with those of *C. tepidum*,[2] which enables us to propose the possible H-bond donors to the carbonyl groups of the *C. tepidum* primary donor. The correlation of the H-bonding pattern of the *C. tepidum* primary donor with physicochemical properties such as the $P°/P^{\bullet+}$ redox midpoint potential and the positive charge distribution in $P^{\bullet+}$ is consistent with previous conclusions concerning histidine H-bonding in the modulation of the redox potential of the primary donor of *Rb. sphaeroides* [Lin et al., 1994; Mattioli *et al*., 1995; reviewed in Allen and Williams (1995)].

Crystals of RCs from *C. tepidum* suitable for X-ray crystallography have been obtained (Kobayashi & Nozawa, 1993) and preliminary crystallographic studies have been recently reported (Katayama *et al*., 1994). The structural model and protein interactions of the primary donor of *C. tepidum* reported here combined with the very recently determined primary protein sequence[2] of the L and M subunits should be very useful in the refining of the three-dimensional RC structure which is currently being solved, especially for assessing the H-bonding interactions in the P microenvironment.

EXPERIMENTAL PROCEDURES

Chromatophores of *C. tepidum* were prepared as previously reported (Nozawa *et al*., 1986). Reaction centers from *C. tepidum* were isolated and purified as described in Nozawa *et al*. (1987); further purification was done as described in Katayama *et al*. (1994), except that final RCs samples were in 20 mM Tris-HCl (pH 8.0) and 0.72% OG detergent. Chromatographic fractions of *C. tepidum* RCs with and without the RC-associated tetraheme cytochrome subunit

[2] The complete protein sequences for the L, M, and cytochrome subunits will be published elsewhere [Nozawa, T. Fathir, I., Yoza, K., Kojima, A., Tanaka, K., Kobayashi, M., Wang, Z.-Y., & Lottspeich, F. (1996) *Photosynth. Res.* (submitted for publication)].

were obtained with final A_{280}/A_{800} ratios of 1.8 and 1.6, respectively (Nozawa *et al*., 1987). These RC samples were concentrated using Centricon 100 microconcentrators (Amicon) to *ca*. 100 OD units at 800 nm for the FT Raman experiments.

Near-infrared FT Raman spectra were recorded using a Bruker IFS 66 interferometer coupled to a Bruker FRA 106 Raman module as described elsewhere (Mattioli *et al*., 1991). The samples were excited with 180 and 200 mW of 1064-nm radiation for room- and low-temperature (10 K) measurements, respectively, which was provided by a diode-pumped Nd:YAG laser; the spectral resolution was 4 cm^{-1}. RC samples were either contained in a sapphire cell for the room-temperature measurements or were immersed in a gas-flow cryostat (SMC-TBT, France) regulated by circulation of cold helium gas for the low-temperature experiments (10 K). For these experiments, RCs were treated with either sodium ascorbate or potassium ferricyanide in order to poise them in their reduced (P°) or oxidized ($P^{\bullet+}$) state, respectively.

Near-infrared room-temperature absorption spectra (700−1300 nm) were recorded with the same FT interferometer described above operating in absorption mode (Wachtveitl *et al*., 1993); 1-mL samples at a final concentration of *ca*. 0.2 OD unit at 800 nm were measured in a 1-cm quartz cuvette. Absorption spectra of P° were obtained from RC samples in the presence of sodium ascorbate while those of $P^{\bullet+}$ were obtained exploiting the actinic effect of the measuring beam as described elsewhere (Mattioli *et al*., 1995).

Anaerobic redox titrations (Dutton & Wilson, 1974) of *C. tepidum* chromatophores were carried out under argon gas in a cuvette containing 2 mL of sample with an optical path length of 1 cm. The photooxidation of P following a saturating laser flash was monitored by the absorbance change at 1283 nm using the apparatus described previously (Venturoli *et al*., 1993). Chromatophore samples were prewashed with 2 mM potassium ferricyanide and used at a final concentration of 5 OD units at 850 nm, in 50 mM MOPS (pH 7.0) and 20 mM KCl. The following redox mediators were used: 1,2-naphthoquinone, 1,4-naphthoquinone, 2,5-dihydroxy-*p*-benzoquinone, 1,2-naphthoquinone-4-sulfonic acid, 1,1′-dimethylferrocene, and *N*,*N*,*N*′,*N*′-tetramethyl-*p*-phenylenediamine at 20 μM and ferrocyanide and ferricyanide at initial concentrations of 20 μM. The potential was varied by additions of ascorbate, ferricyanide, or porphyrexide (4-amino-2,5-dihydro-2-imino-5,5-dimethyl-1*H*-imidazol-1-yloxy; which was a kind gift from Dr. A. W. Rutherford). For measurement of ambient redox potential, a platinum electrode and a calomel reference electrode (saturated KCl) were used. The electrode was calibrated with a quinhydrone reference in 0.01 N HCl and 0.09 M KCl at pH 2.098 with a potential of +575 mV versus standard hydrogen electrode at 25 °C (Clark, 1960).

Potentiometric titration of *C. tepidum* RCs with and without tetraheme cytochrome *c* subunit were carried out in an ultrathin path length (70 μm) cuvette composed of ITO (indium titanium oxide) and normal glass, with a Teflon spacer (50 μm thick) in between them. The cuvette has a small reference electrode of Ag/AgCl and Pt wire as the counterelectrode. A potentiometer (Hokuto Denko, HAB-151) was used to vary the potential in 10-mV steps; the absorption changes at *ca*. 880 nm and the steady-state spectra were measured with a Shimadzu UV 3100 spectrometer; 150-μL RC samples in 15 mM sodium phosphate buffer (pH = 7.0), 0.8% OG, and 60 mM KCl were measured at a final concentration of *ca*. 60 μM.

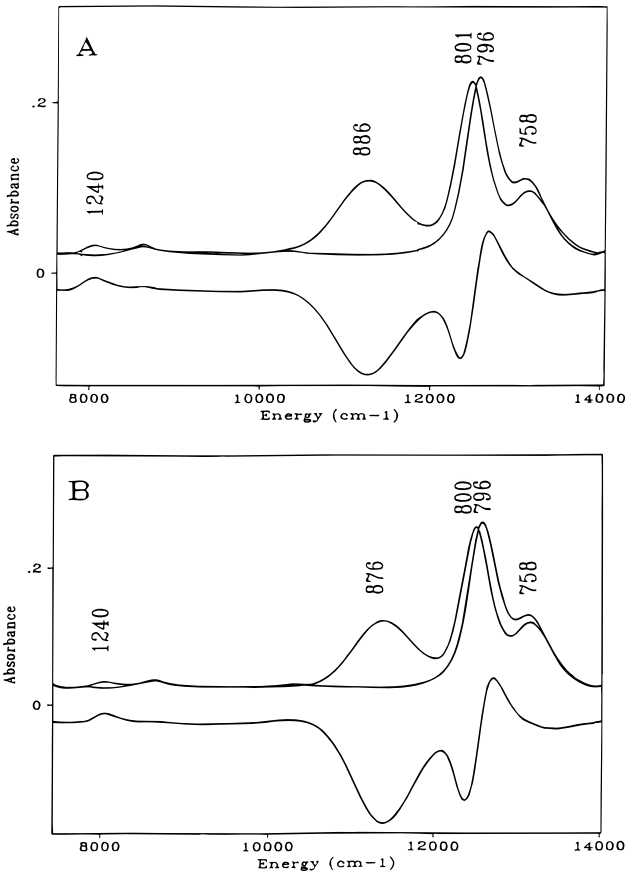

FIGURE 1: Near-infrared absorption spectrum of *C. tepidum* reaction centers with the bound tetraheme cytochrome (panel A) and devoid of the cytochrome subunit (panel B). Spectra of reduced and oxidized RCs are shown in each panel, together with their respective computed oxidized-minus-reduced spectra (bottom). The peak positions are labeled in nanometer units. The band at *ca*. 1150 nm in both reduced and oxidized spectra does not arise from the primary donor. Conditions: coaddition of 250 interferograms; room temperature. Spectral resolution was 2 cm^{-1}.

For all titrations, the data were fit by the Nernst equation with fixed $n = 1$.

RESULTS

The near-infrared electronic absorption spectra for reduced (P°) and oxidized ($P^{\bullet+}$) *C. tepidum* RCs with (panel A) and without (panel B) the associated tetraheme cytochrome are shown in Figure 1, as well as the calculated difference spectra. These spectra resemble that of *Rb. sphaeroides* RCs (Nozawa *et al*., 1987; Garcia *et al*., 1987). A significant red shift of 10 nm is observed for the lower excitation P Q_y band (886 nm; Figure 1, panel A) in RC samples which possess the associated tetraheme cytochrome, as was previously reported (Nozawa *et al*., 1987). Upon oxidation, the 886-nm (panel A) and 876-nm (panel B) absorption bands bleach, while a new band at 1240 nm appears in the absorption spectrum of both RC samples; the latter is reminiscent of the $P^{\bullet+}$ band (1248 nm) in the oxidized RCs from *Rb. sphaeroides* (Wachtveitl *et al*., 1993) although significantly blue-shifted by 8 nm. As well, the electrochromic shift of the 796-nm absorption band corresponding to the accessory BChl molecules appears to be slightly greater

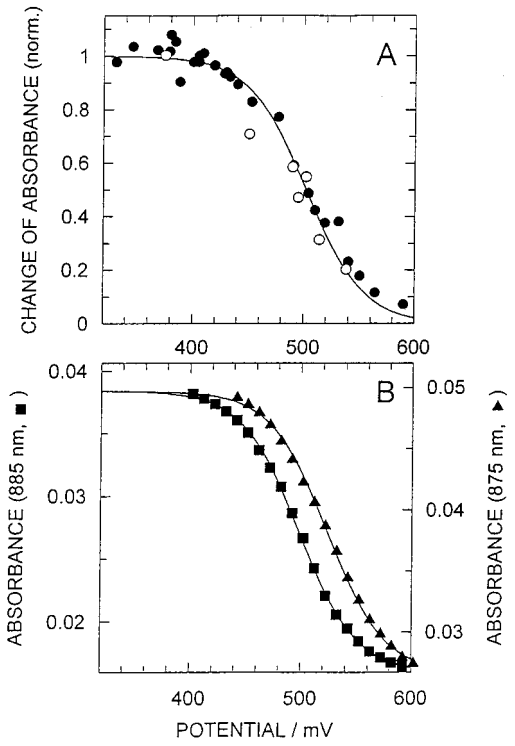

FIGURE 2: (A) Effect of ambient redox potential on the amplitude of photooxidation of P in chromatophore samples, induced by a saturating laser flash monitored at 1283 nm. Data are normalized to maximum signals as determined from the fitted curve. Data points were fit by the Nernst equation with $n = 1$ (solid line) yielding an $P°/P^{•+}$ redox midpoint potential (E_m) of $+(502 \pm 10)$ mV. Data from oxidative titrations are indicated by filled circles (●) and those from reductive titrations by open circles (○). (B) Redox titration of P in isolated RCs with the associated tetraheme *c*-type cytochrome subunit (filled squares, ■) and RCs devoid of it (filled triangles, ▲). Both set of data points were fitted by the Nernst equation (solid lines) yielding $P°/P^{•+}$ redox midpoint potentials of $+(497 \pm 5)$ and $+(526 \pm 5)$ mV for RCs with and without the tetraheme cytochrome subunit.

for the RC sample possessing the associated tetraheme cytochrome.

The chemical and electrochemical redox titrations for the chromatophores and isolated reaction centers are shown in Figure 2. The $P°/P^{•+}$ redox midpoint potentials of isolated *C. tepidum* RCs with and without the associated tetraheme cytochrome as well as in chromatophores were determined to be $+(497 \pm 5)$, $+(526 \pm 5)$, and $+(502 \pm 10)$ mV, respectively, versus NHE.

The assignments of the 12 π-conjugated carbonyl vibrators corresponding to the resonance Raman spectra (under various excitation conditions) of the six bacteriochlorin pigments in the RC of *Rb. sphaeroides* have been previously tabulated in the literature (Robert & Lutz, 1988; Lutz & Robert, 1988; Robert 1990; Palaniappan *et al*., 1993). The selective resonance Raman vibrational spectrum of reduced P from these RCs has been observed using excitation wavelengths in the near-infrared spectral region at ca. 860 nm (i.e., Q_y resonance conditions with the 860-nm absorption band of P) (Shreve *et al*., 1991; Palaniappan *et al*., 1992) and carbonyl vibrators of P have been assigned (Palaniappan *et al*., 1993). However, the FT Raman technique using 1064-nm excitation permits the selective observation of the P carbonyl vibrators in both the P° and $P^{•+}$ states with little or no interference from P fluorescence and high signal-to-noise (Mattioli *et al*., 1991, 1993). Comparison of the FT

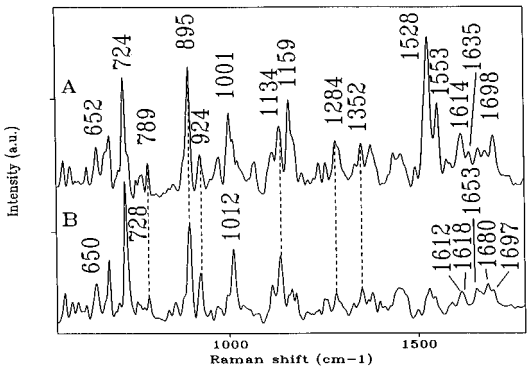

FIGURE 3: Low temperature (10 K) Fourier transform (FT) preresonance Raman spectra of *C. tepidum* RCs (A) and *Rb. sphaeroides* RCs (B) poised with 10 mM sodium ascorbate and excited at 1064 nm with 200 mW of Nd:YAG laser power. The spectral resolution was 4 cm^{-1} and each spectrum results from the coaddition of 6000 interferograms.

Raman spectra of *C. tepidum* RCs in their P° and $P^{•+}$ states with those from *Rb. sphaeroides* will be discussed below.

The low-temperature FT preresonance Raman spectrum (excited with 1064-nm radiation) of *C. tepidum* cytochrome-free RCs reduced by ascorbate is shown in Figure 3A, together with that for *Rb. sphaeroides* (Figure 3B). These spectra exhibit no contributions from the sapphire cell (see Experimental Procedures), in particular the sapphire Raman band at *ca*. 645 cm^{-1}, which masks the BPhe *a* band at *ca*. 650 cm^{-1} (Mattioli *et al*., 1991). The room-temperature FT Raman spectrum of *Rb. sphaeroides* RCs was previously reported (Mattioli *et al*., 1991). The bands at 728, 895, 1012, 1134, and 1528 cm^{-1} were reported as marker bands of BChl *a* species while those at 650 and 1583 cm^{-1} correspond to BPhe *a* contributions (Mattioli *et al*., 1991). The FT Raman spectra of *C. tepidum* and *Rb. sphaeroides* RCs in Figure 3 (panels A and B, respectively) are similar, and the intensity ratios of the BChl to BPhe marker bands are comparable, indicating that the pigment composition of these two RCs is similar and that the 1064-nm excitation results in comparable preresonance enhancements of the pigments. Significant differences between these two FT Raman spectra (Figure 3) are noted by the presence of relatively intense bands at 1553, 1528, 1159, and 1001 cm^{-1} for the *C. tepidum* RC which are not observed for the *Rb. sphaeroides* carotenoidless R 26 strain RC. However, the approximate frequencies and relative intensities of these FT Raman bands resemble those seen in the FT Raman spectrum of RCs from the carotenoid-containing *Rb. sphaeroides* 2.4.1 strain (Mattioli *et al*., 1993); a calculated difference between the FT Raman spectrum of reduced *Rb. sphaeroides* RCs of the carotenoid-containing 2.4.1 strain from that of the carotenoidless R 26 strain yielded positive bands at 1564, 1528, 1167, 1158, and 1005 cm^{-1}, among other weaker ones, all attributable to the carotenoid in the 2.4.1 reaction center (Mattioli *et al*., 1993). Thus the bands seen at 1553, 1528, 1159, and 1001 cm^{-1} in the FT Raman spectrum of the *C. tepidum* RCs are most likely arising from the RC-bound carotenoid. The chemical identity and configuration of this carotenoid is not presently known. Comparing the FT Raman spectra of the *C. tepidum* and *Rb. sphaeroides* R 26 RCs, one also notes that the intensity of the 895-cm^{-1} band relative to that of the ca. 725-cm^{-1} band is greater for the case of *C. tepidum*. Both bands arise from BChl (Mattioli *et al*., 1991, 1993). The extra intensity at

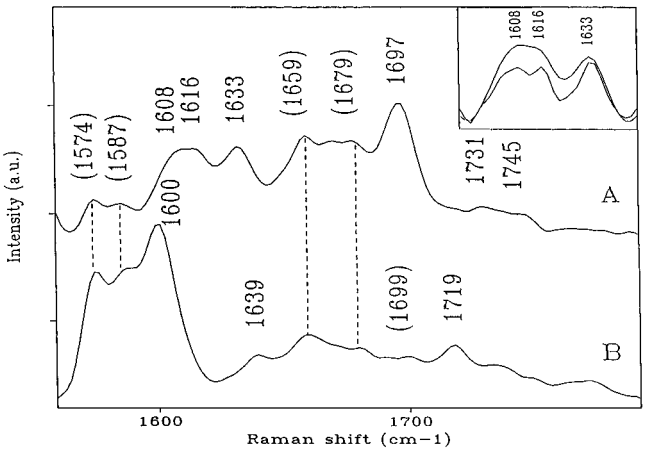

FIGURE 4: Room-temperature FT (pre)resonance Raman spectra of reduced (A) and oxidized (B) RCs from *C. tepidum* without bound tetraheme cytochrome, showing the carbonyl region. Coaddition of 8000 interferograms and 180-mW power of 1064-nm radiation were used. Spectral resolution was 4 cm^{-1}. The peak positions were obtained by Fourier deconvolution and second derivative analysis. The bands displayed in parentheses do not arise from P° or $P^{\bullet+}$ contributions. The inset shows an expanded view of the 1600−1640-cm^{-1} region of the reduced RCs spectrum (A) together with its Fourier deconvoluted spectrum.

895 cm^{-1} has been observed in the FT Raman spectrum from antenna complexes of BChl *a* type either containing or not containing a carotenoid (Mattioli *et al*., 1993), and is also observed in *C. vinosum* RCs (Ivancich and Mattioli, unpublished data). The vibrational stretching modes of the bacteriochlorin π-conjugated carbonyl groups contribute in the high-frequency region 1620−1710 cm^{-1} (Lutz, 1984). Comparing Figure 3, panels A and B, in this spectral region, differences are observed for the conjugated carbonyl frequencies of the BChl molecules bound in *C. tepidum* and *Rb. sphaeroides*, indicating significant changes for these two species in the protein interactions of the BChl conjugated carbonyl groups (see below).

Due to the similarity in the Q_y absorption bands of the primary donors of *C. tepidum* (876 nm) and *Rb. sphaeroides* (865 nm), it is reasonable to expect a similar selective preresonance Raman enhancement of P in the carbonyl region of the FT Raman spectrum of the *C. tepidum* RCs excited with 1064-nm radiation. An equivalent situation was found for other BChl *a*-containing RCs to which FT Raman spectroscopy using 1064-nm excitation was applied for deducing their primary donor structure and their protein interactions (Agalidis *et al*., 1992; Feiler *et al*., 1995; Ivancich *et al*., 1996). In all these cases, as well as for *Rb. sphaeroides* RCs (Mattioli *et al*., 1991, 1994), a preresonance Raman vibrational spectrum of neutral P (P°) was obtained via the 1064-nm excitation of the FT Raman spectrum of reduced RCs, while a genuine resonance Raman spectrum of $P^{\bullet+}$ could be observed upon oxidation.

The room-temperature FT Raman spectra of *C. tepidum* RCs (devoid of the cytochrome subunit) excited with 1064-nm radiation are shown in Figure 4 for both their reduced P° (Figure 4A) and oxidized $P^{\bullet+}$ (Figure 4B) states. The spectrum in Figure 4A exhibits three evident bands at *ca*. 1612, 1633, and 1697 cm^{-1}. The band centered at *ca*. 1612 cm^{-1} is broad (24 cm^{-1} FWHM), while the 1697-cm^{-1} band is narrow (14 cm^{-1} FWHM) and twice as intense as the others in the carbonyl region. Fourier deconvolution and second derivative analyses (not shown) of the broad band centered at *ca*. 1612 cm^{-1} clearly indicates that there are two components at 1608 and 1616 cm^{-1} (see inset of Figure 4). Such closely unresolved bands have been observed in the FT Raman spectrum of RCs from *Rvx. gelatinosus* (Agalidis *et al*., 1992). The bands at 1616, 1633, and 1697 cm^{-1} clearly disappear upon oxidation of the RCs to their $P^{\bullet+}$ state (Figure 4B) and thus are attributable to P°. Other bands observed in Figure 4A are those at 1659 and 1679 cm^{-1}, which persist in the spectrum of Figure 4B and thus cannot be ascribed to P°; the band at 1659 cm^{-1} probably arises from the protein and/or accessory BChls (Mattioli *et al*., 1991, 1994), while the 1679-cm^{-1} band could arise from the BPhe molecules (Mattioli *et al*., 1994; Ivancich *et al*., 1996). Two other weak bands at 1731 and 1745 cm^{-1} resemble those observed in the FT Raman spectrum of P° of *Rb. sphaeroides*, attributable to the C_{10} carbomethoxy ester carbonyls (Mattioli *et al*., 1991).

Obvious new bands which appear upon $P^{\bullet+}$ formation are those at 1600, 1639, and 1719 cm^{-1} (Figure 4B); these bands are attributable to $P^{\bullet+}$ and are resonantly enhanced via the 1240-nm absorption band of this species (Figure 1). As mentioned above, the 1659- and 1679-cm^{-1} bands were also present in the P° spectrum of Figure 4A and thus not attributable to $P^{\bullet+}$. The weak band at 1699 cm^{-1} cannot be unambiguously assigned to $P^{\bullet+}$ as it may have been masked underneath the intense 1697-cm^{-1} band in the P° spectrum. These bands not attributable to $P^{\bullet+}$ are similar to those seen in the $P^{\bullet+}$ spectrum of *Rb. sphaeroides* (Mattioli *et al*., 1991). The 1659-cm^{-1} band most probably arises from BChl molecules other than the primary donor or protein contributions (Mattioli *et al*., 1994, 1995; Beekman *et al*., 1995). The 1679-cm^{-1} band could arise from BPhe molecules contributions, similar to those observed in the FT Raman spectrum of *Cf. aurantiacus* RCs at *ca*. 1680 cm^{-1}, in both the reduced and oxidized states (Ivancich *et al*., 1996).

The Primary Donor. From the above discussion, we assign the 1608-, 1616-, 1633-, and 1697-cm^{-1} FT Raman bands in Figure 4A to P° of the *C. tepidum* RC. The 1608-cm^{-1} band is attributable to a BChl C_aC_m methine bridge stretching mode indicating pentacoordination [i.e., one axial ligand; Cotton and Van Duyne (1981)]. This band is reminiscent of that observed in FT Raman spectra of BChl *a*-containing RCs (Mattioli *et al*., 1992a) where the sole narrow band at 1607 cm^{-1} indicated that both BChl constituents possessed a single axial ligand each. The crystal structure of the RCs from *Rb. sphaeroides* revealed that His L173 and His M202 were the axial ligands for each BChl molecule of the primary donor (El-Kabbani *et al*., 1991; Chirino *et al*., 1994; Ermler *et al*., 1994). The 1608-cm^{-1} band observed for P° of the *C. tepidum* RC also indicates that it arises from a single population of BChl *a* molecules and its frequency indicates that these BChl *a* molecules possess one axial ligand each. There is no observable band at ca. 1597 cm^{-1} which would indicate the enhancement of Raman contributions from a BChl *a* molecule possessing two axial ligands (Mattioli *et al*., 1991). The other bands observed in Figure 4A vibrating at 1616, 1633, and 1697 cm^{-1} can be assigned to π-conjugated carbonyl groups (Lutz *et al*., 1984; Mattioli *et al*., 1991; Agalidis *et al*., 1992). A BChl molecule possesses two conjugated carbonyl groups, so the fact that there are at least three carbonyl vibrational bands in Figure 4A indicates that the primary donor of *C. tepidum* should be constituted of more than one BChl

molecule, most probably two, as is the case for *Rb. sphaeroides* (Mattioli *et al*., 1991) and other purple bacterial species (Mattioli *et al*., 1992a). Thus, presuming that the primary donor of the *C. tepidum* is indeed a dimer (Nozawa *et al*., 1987; Kobayashi *et al*., 1996), then each of the BChl constituents possess one axial ligand.

In vitro studies on BChl *a* molecules (Lutz *et al*., 1984), have shown that the C_2 acetyl carbonyl groups can vibrate in the frequency range of *ca*. 1620−1660 cm^{-1}, depending if they are hydrogen-bonded or not; similarly, the C_9 keto carbonyls are observed to vibrate between *ca*. 1660 and *ca*. 1700 cm^{-1}. In both cases, the magnitude of the shift reflects the strength of the H-bond. Considering these arguments, (i) the 1616- and the 1633-cm^{-1} bands from the spectrum in Figure 4A can be unambiguously attributed to the two C_2 acetyl carbonyl groups of each BChl molecule constituting P° (see above), both hydrogen-bonded but with different H-bond strengths, and (ii) the 1697-cm^{-1} band should correspond to a C_9 keto carbonyl group, free of interactions. With three bands attributed to the conjugated carbonyl groups of P°, the fourth band corresponding to the other keto carbonyl is unaccounted for. Based on the large relative intensity of the 1697-cm^{-1} band, we propose that both C_9 keto carbonyls contribute to this single Raman band and are vibrationally indistinguishable. The 1616-cm^{-1} band is quite low in frequency, indicating a stronger H-bond than that observed in *Rb. sphaeroides* (vibrating at 1620 cm^{-1}) but similar to that observed for P° of *Rvx. gelatinosus* (Agalidis *et al*., 1992). The 1633-cm^{-1} band of *C. tepidum* compared to the 1653-cm^{-1} band corresponding to the free acetyl carbonyl of P_M of *Rb. sphaeroides* is downshifted by 20 cm^{-1}. This downshift is probably too large to be entirely due to local dielectric effects in the protein near the acetyl carbonyl. The frequency of chlorophyll carbonyl groups can vary as much as 15 cm^{-1} depending on the dielectric properties of the medium (Koyama *et al*., 1986; Krawczyk, 1989). Palaniappan and Bocian (1995) have reported bacteriopheophytin carbonyl frequency shifts of 14 cm^{-1} in a mutant reaction center of *Rb. capsulatus*.

In summary, from the analysis of the FT Raman spectra of *C. tepidum* RCs (Figure 4) the following H-bond pattern for the primary donor in its neutral ground state is proposed: (i) both C_2 acetyl carbonyl groups are H-bonded but experience different hydrogen-bond strengths and (ii) the C_9 keto carbonyl groups are both free of interactions and exhibit very similar vibrational frequencies. These results differ from those obtained for *Rb. sphaeroides* RCs, where only the P_L C_2 acetyl carbonyl is H-bonded (to His L168) and the non-H-bonded C_9 keto carbonyl groups exhibit significantly different vibrational frequencies (Mattioli *et al*., 1991, 1994).

The FT Raman spectra of *C. tepidum* RCs containing the associated tetraheme cytochrome were also recorded in their P° and $P^{\bullet+}$ states, in the presence of ascorbate and ferricyanide, respectively (data not shown). Comparison of these spectra with those of *C. tepidum* RCs devoid of the tetraheme cytochrome did not reveal any significant difference in terms of band relative intensity changes, for both their respective P° and $P^{\bullet+}$ spectra. Also, within the instrumental error (±1 cm^{-1}), the carbonyl band frequencies are not observed to shift between RC samples with and without the associated tetraheme subunit, indicating that there are no measurable conformational differences in the microenvironment of P between these samples.

The Oxidized Primary Donor. The 1600-, 1639-, and 1719-cm^{-1} bands in Figure 4B are assigned to $P^{\bullet+}$. These bands are reminiscent of those observed in the FT Raman spectrum of *Rb. sphaeroides* RCs at 1600, 1641, and 1717 cm^{-1} (Mattioli *et al*., 1991, 1994). In the case of *Rb. sphaeroides* the bands were assigned to the C_aC_m stretching mode, which, upon P oxidation, downshifted from 1607 cm^{-1}, and to the C_2 acetyl and C_9 keto carbonyl groups of P_L, which upshifted from 1620 and 1691 cm^{-1}, respectively (Mattioli *et al*., 1991). Under similar considerations, the 1600-cm^{-1} band in Figure 4B can be attributed to the downshifted vibrational frequency of the band arising from the C_aC_m methine bridge stretching modes (band at 1608 cm^{-1} in the P° FT Raman spectrum, Figure 4A), and that observed at 1719 cm^{-1} should correspond to one of the C_9 keto carbonyl groups of P which upshifted 22 cm^{-1}; both shifts result from the oxidation of the primary donor of *C. tepidum*. The 1639-cm^{-1} band in Figure 4B could be ascribed, in analogy to *Rb. sphaeroides* (Mattioli *et al*., 1991), to that of a shifted C_2 acetyl carbonyl upon oxidation. Since a 6-cm^{-1} upshift, upon P oxidation, of the C_2 acetyl vibrating at 1633 cm^{-1} (see Figure 4A) would be too small as compared to the observed upshift (11 cm^{-1}) for *in vitro* BChl a^+ molecules (Mäntele *et al*., 1988), the only plausible candidate for this 1633-cm^{-1} band is the C_2 acetyl carbonyl vibrating at 1616 cm^{-1} in the P° spectrum (see Figure 4A). Then the observed upshift upon oxidation is 23 cm^{-1}, very similar to the case of P_L C_2 acetyl carbonyl in *Rb. sphaeroides*.

DISCUSSION

Structure of the Primary Donor of C. tepidum. The results presented in this work indicate that although the basic structure of the primary donor of the purple sulfur bacterium *C. tepidum* is similar to that of the purple non-sulfur bacterium *Rb. sphaeroides*, interesting differences in the H-bonding pattern and protein interactions are observed. In particular, we propose that the primary donor of *C. tepidum* is constituted of two BChl *a* molecules with one axial ligand each, as in the case of *Rb. sphaeroides* (Mattioli *et al*., 1991), although the H-bond patterns of the π-conjugated carbonyl groups of these BChl molecules exhibit subtle differences (Figure 5). The C_2 acetyl carbonyls of the *C. tepidum* primary donor are both H-bonded, and the C_9 keto carbonyls are both free from interactions. Specific assignments for the vibrational frequencies of the C_2 acetyl and the C_9 keto carbonyl groups to those of the P_L and P_M constituents of the primary donor of *C. tepidum* may be accomplished by comparison of the primary sequences of the L and M protein subunits of its RC with those of *Rb. sphaeroides* and *Rps. viridis* (Table 1).

The strongly conserved His L173 and His M202 residues [see Figure 1 in Nagashima *et al*. (1993) and Figure 9 in Nagashima *et al*. (1994)] which serve as the axial ligands to the primary donor of *Rb. sphaeroides* (El-Kabbani *et al*., 1991; Chirino *et al*., 1994; Ermler *et al*., 1994) are also conserved in *C. tepidum* RC (Table 1). Thus, His L181 and His M201 should be the sole axial ligands to each Mg atom of the P_L and P_M molecules, respectively, of *C. tepidum* (Figure 5).

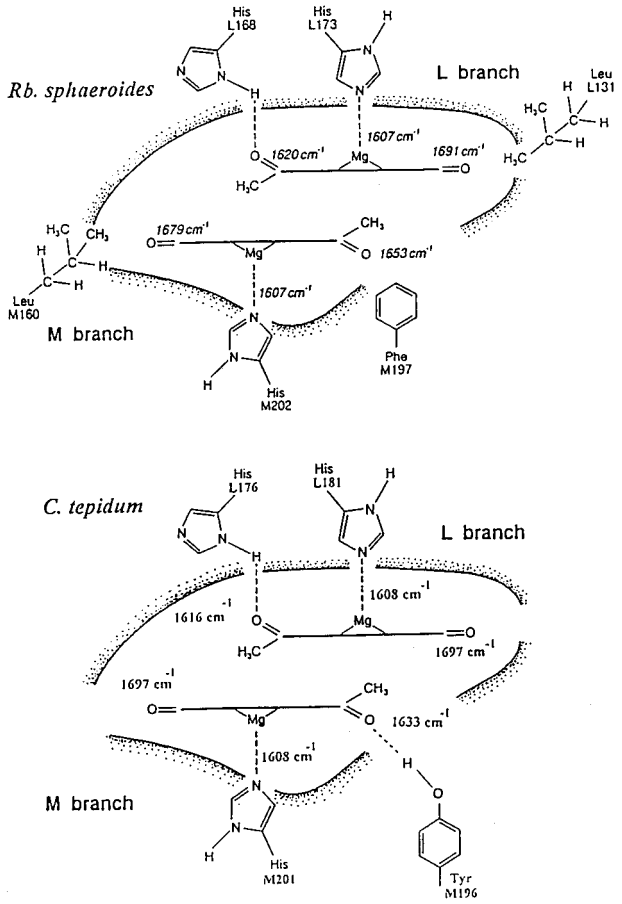

FIGURE 5: Comparison of schematic diagrams exhibiting the microenvironments (top) of the primary donor of *Rb. sphaeroides* (Mattioli *et al*., 1994) and (bottom) of the proposed structural model for *C. tepidum* RCs as deduced from FT Raman data and sequence alignments. The assigned conjugated carbonyl frequencies are also noted.

Table 1: Sequence Alignment of the L and M Subunits of the RCs from *C. tepidum*, *Rb. sphaeroides*, and *Rps. viridis*[e]

Rps. viridis[a]	L126	F	M	F	C	V	L	Q	V	F	R	P	L136
Rb. sphaeroides[b]	L126	L	A	Y	L	T	L	V	L	F	R	P	L136
C. tepidum[c]	L134	G	A	Y	L	V	L	V	F	V	R	P	L144
Rps. viridis[a]	L165	L	N	W	**H**	Y	N	P	G	**H**	M	S	L175
Rb. sphaeroides[b]	L165	G	N	F	**H**	Y	N	P	A	**H**	M	I	L175
C. tepidum[c]	L173	L	H	F	**H**	Y	N	P	A	**H**	M	L	L183
C. tepidum[c]	M154	F	F	Y	L	V	L	G	F	I	R	P	M164
Rb. sphaeroides[d]	M155	W	L	W	M	V	L	G	F	I	R	P	M165
Rps. viridis[a]	M153	F	F	V	L	C	I	G	C	I	H	P	M163
C. tepidum[c]	M193	G	N	L	**Y**	Y	N	P	F	**H**	M	L	M203
Rb. sphaeroides[d]	M194	G	N	L	**F**	Y	N	P	F	**H**	G	L	M204
Rps. viridis[a]	M192	G	N	F	**Y**	Y	C	P	W	**H**	G	F	M202

[a] From Michel *et al*. (1986). [b] From Williams *et al*. (1984). [c] This work. [d] From Williams *et al*. (1983). [e] The amino acid residues designated in underlined boldface type correspond to the position of His L173 and His M202 in *Rb. sphaeroides*. Those designated in boldface type correspond to the position of His L168 and Phe M197 in *Rb. sphaeroides* which are related to the H-bonded P_L C_2 acetyl carbonyl and the free P_M C_2 acetyl carbonyl groups, respectively (Mattioli *et al*., 1994).

From the FT Raman spectrum of *C. tepidum* RCs, both C_2 acetyl carbonyl groups, vibrating at 1616 and 1633 cm^{-1}, are H-bonded. Similar measurements on *Rb. sphaeroides* RCs showed that the P_L C_2 carbonyl group, vibrating at 1620 cm^{-1}, is H-bonded (to His L168), while the P_M C_2 acetyl carbonyl vibrating at 1653 cm^{-1} is free from interactions (Mattioli *et al*., 1991, 1994). Moreover, in the FT Raman spectrum of mutant RCs from *Rb. sphaeroides* in which Phe M197 was genetically replaced by a His or a Tyr residue (both being potential H-bond donors) the 1653-cm^{-1} band was observed to downshift to 1630 or 1636 cm^{-1}, respectively; this effect was interpreted in both cases as the formation of a H-bond on the P_MC_2 acetyl carbonyl group (Mattioli *et al*., 1994; Wachtveitl *et al*., 1993). A similar lower vibrational frequency (1632 cm^{-1}), as compared to the 1653-cm^{-1} band in the FT preresonance Raman spectrum of *Rb. sphaeroides* RCs, was observed for the native RC from *Cf. aurantiacus* (Ivancich *et al*., 1996) and was assigned to the H-bonded P_M C_2 acetyl carbonyl group, the proposed H-bond donor being a tyrosine residue (Tyr M187) at the analogous position of Phe M197 of *Rb. sphaeroides* (Shiozawa *et al*., 1989).

The sequence alignment for the M subunit of *C. tepidum*, *Rb. sphaeroides*, and *Rps. viridis* (Table 1) shows that for *C. tepidum* RCs the amino acid residue at the equivalent position of Phe M197 (in *Rb. sphaeroides*) is a tyrosine (Tyr M196), as it is for *Rps. viridis* and *Cf. aurantiacus* (see above). The crystal structure of the *Rps. viridis* RC shows that Tyr M195 forms a H-bond to the acetyl carbonyl of ring I in P_M (Deisenhofer & Michel, 1989; Deisenhofer *et al*., 1995). Thus, we propose that the P_M C_2 acetyl carbonyl group vibrating at 1633 cm^{-1} in *C. tepidum* RC is hydrogen-bonded to Tyr M196 (Figure 5).

The other H-bonded C_2 acetyl carbonyl group from the primary donor of *C. tepidum* that is observed to vibrate at 1616 cm^{-1} (Figure 4A) is then assigned to P_L. The sequence alignment of the L subunits in Table 1 shows that *C. tepidum* possesses also a histidine residue (His L176) at the equivalent position of His L168 in *Rb. sphaeroides* and *Rps. viridis*; this histidine residue is strongly conserved in other species [see Figure 9 in Nagashima *et al*. (1994)] and forms the H-bond in *Rb. sphaeroides* and *Rps. viridis* with the primary donor, as revealed by the crystal structures (see above). Thus, a similar H-bond is expected for the P_L C_2 acetyl carbonyl group in *C. tepidum* RC donated by His L176 (Figure 5). It is noteworthy that the observed vibrational frequency (1616 cm^{-1}) is 4 cm^{-1} lower than that observed for the P_L C_2 acetyl carbonyl in the FT preresonance Raman spectrum of *Rb. sphaeroides* RCs (Mattioli *et al*., 1991, 1994) indicating a stronger H-bond in the *C. tepidum* primary donor. In fact, other purple bacterial RCs exhibit a 1620-cm^{-1} band as in *Rb. sphaeroides* (Mattioli *et al*., 1992a) except for the primary donor of *Rvx. gelatinosus*, for which the P_L C_2 acetyl carbonyl is observed to vibrate, as in the case of *C. tepidum* P, at 1616 cm^{-1} (Agalidis *et al*., 1992). Accordingly, the sequence alignment for the L subunits of several bacterial RCs [see Figure 9 in Nagashima *et al*. (1994)] shows that only *Rvx. gelatinosus* and *Roseobacter* (*Ro.*) *denitrificans* have a histidine residue instead of an asparagine at the equivalent position of Asn L166 in *Rb. sphaeroides*, *Rb. capsulatus*, and *Rhodospirillum rubrum*. Interestingly, the equivalent amino acid residue for *C. tepidum* RC at the position L166 in *Rb. sphaeroides* is also a histidine (His 174, Table 1). A histidine residue at this position could influence the H-bond between His L168 and P_L.

Conformational changes on the primary donor of *Rb. sphaeroides* RCs were observed as a result of lowering the temperature from 300 to 10 K (Mattioli *et al*., 1992b; Ivancich, Lutz, and Mattioli, unpublished results). These changes were detected by the 2-cm^{-1} downshift of the P_L C_2 acetyl carbonyl band (1620 cm^{-1} at 300 K down to 1618 cm^{-1} at 10 K) and the 6 cm^{-1} upshift of the P_L C_9 keto carbonyl band (1691 cm^{-1} at 300 K to 1697 cm^{-1} at 10 K) (see Figure 2B). These conformational changes can be interpreted as an induced repositioning of the carbonyl groups with respect to the protein so that their mutual interactions change, as reflected by the change in vibrational frequency. For *C. tepidum* RCs, a 2-cm^{-1} downshift is also observed for the P_L C_2 acetyl carbonyl band while only a 1-cm^{-1} shift is observed for the 1697-cm^{-1} band arising from the C_9 keto carbonyl (compared Figures 3A and 4A); this indicates that the repositioning of the BChl molecules constituting P of *C. tepidum* RCs is attenuated in comparison with *Rb. sphaeroides*, at least at the level of the P_L C_9 keto carbonyl group.

As mentioned before, room-temperature FT Raman spectra of RC samples both with and without cytochrome show very similar vibrational frequencies for the four carbonyl groups of P. Under similar considerations as for the temperature dependence studies, the invariance of the P-conjugated carbonyl group frequencies in both cytochrome-free and cytochrome-containing RCs enables us to conclude that no significant conformational changes with respect to repositioning of the $(BChl)_2$ occur due to the presence of the tightly bound tetraheme cytochrome subunit in *C. tepidum* RCs. Thus, the 10-nm red shift of the electronic absorption band for the primary donor of RC samples that contain the cytochrome subunit as compared to those devoid of it (see Figure 1) probably arises largely from electrostatic effects and not necessarily from conformational changes induced by the tetraheme subunit, as previously suggested (Nozawa *et al*., 1987). Nevertheless, we cannot exclude the possibility that the BChl molecules constituting the primary donor could come closer together, provided that no repositioning of the conjugated carbonyl groups with respect to the protein occurs. Interestingly, the $P^{\bullet+}$ electronic absorption band is the same for both samples with or without the tetraheme cytochrome subunit.

The Oxidized Primary Donor. Vibrational spectroscopy, and in particular resonance Raman spectroscopy, is a useful technique in analyzing the extent of charge distribution in porphyrin radical complexes (Donohoe *et al*., 1988; Duchowski & Bocian, 1990; Tran-Thi *et al*., 1994). As previously discussed (Mattioli *et al*., 1991, 1994, 1995), the upshift of the P_L C_9 keto carbonyl band in the FT (pre)resonance Raman spectrum of *Rb. sphaeroides* RCs upon oxidation can be used to estimate the degree of positive charge localization on the P_L molecule of the primary donor. Considering that a non-H-bonded keto carbonyl group of monomeric BChl a^+ *in vitro* upshifts 32 cm^{-1} (Cotton *et al*., 1980; Mäntele *et al*., 1988; Heald & Cotton, 1990) and representing a 100% localization over one BChl molecule, then the observed upshift for the P_L C_9 keto carbonyl group in *Rb. sphaeroides* RC upon oxidation (from 1691 to 1717 cm^{-1}) results in an estimated *ca*. 80% positive charge localization in favor of P_L (Mattioli *et al*., 1991). This analysis assumes that the observed carbonyl frequency shift is linear with charge localization and that no other BChl structural changes affecting the C_9 keto carbonyl frequency occur as a result of P oxidation. Similarly, the 22-cm^{-1} upshift of the P_L C_9 keto carbonyl group of *C. tepidum* RCs upon oxidation (see Figure 4) implies a *ca*. 69% localization of the unpaired electron spin density on one of the BChl molecules of P. Since both keto carbonyls are non-H-bonded and vibrating at the same frequency, we cannot assess from the spectrum which of them has upshifted. But we can confidently attribute the C_2 acetyl carbonyl of P_L as that vibrating at 1616 cm^{-1} in the P° spectrum which upshifts to 1639 cm^{-1} in the $P^{\bullet+}$ spectrum. This indicates that the P_L molecule is selectively resonantly enhanced in the FT Raman spectrum of $P^{\bullet+}$, as was observed in the $P^{\bullet+}$ spectrum of *Rb. sphaeroides* (Mattioli *et al*., 1991). Thus, on the basis of the observed 1639-cm^{-1} band in Figure 4B, the upshifted C_9 keto carbonyl (1719 cm^{-1}) in the $P^{\bullet+}$ spectrum is identified as that of P_L (Mattioli *et al*., 1991). Therefore we estimate that 69% localization of the positive charge is in favor of P_L. This result indicates that the positive charge is more delocalized over both BChl molecules constituting the *C. tepidum* primary donor than it is for *Rb. sphaeroides*.

Interestingly, in a mutant RC from *Rb. sphaeroides* for which a new H-bond was formed on the P_L C_9 keto carbonyl by introducing a Tyr residue at the position of Phe L197 (Wachtveitl *et al*., 1993), an estimated increase of *ca*. 10% of the positive charge localization on P_L was observed and correlated with the 12-nm red shift in the NIR $P^{\bullet+}$ absorption band (from 1248 to 1260 nm). In contrast, the present results show that, for *C. tepidum* RC, the NIR $P^{\bullet+}$ band is 8−10 nm blue-shifted (1240 nm) as compared to that of *Rb. sphaeroides* (Wachtveitl *et al*., 1993; Mattioli *et al*., 1995) and accordingly, the positive charge appears to be 10% less localized on P_L upon oxidation than it is for *Rb. sphaeroides*. A similar trend was observed for the *Rb. sphaeroides* mutant RC in which the Ser L244 was genetically replaced by a Gly (Wachtveitl *et al*., 1993). Taken together, these results imply that factors other than a H-bond between the P_M acetyl carbonyl and a tyrosine residue at the analogous M197 position in *Rb. sphaeroides* contribute to the $P^{\bullet+}$ near-infrared absorption band and the charge localization in this radical cation.

P°/P$^{\bullet+}$ Redox Midpoint Potential. The P°/$P^{\bullet+}$ redox midpoint potential has been shown to correlate to the number and strength of histidine-donated H-bonds (Mattioli *et al*., 1995; Allen & Williams, 1995). Dramatic changes of this potential were observed in mutant RCs constructed to add or remove H-bonds donated by histidine residues on the primary donor (Lin *et al*., 1994); in particular, for the single mutation which results in the formation of a H-bond on the P_M C_9 keto carbonyl group [FH(M197)] in the primary donor of *Rb. sphaeroides* a *ca*. 125-mV increase in the P°/$P^{\bullet+}$ redox midpoint potential was observed. More relevant to the present work are the results on the mutant RC form *Rb. sphaeroides* in which the Phe M197 was genetically replaced by a Tyr residue, FY(M197) (Wachtveitl *et al*., 1993), in this case, the redox potential increased only by *ca*. 25 mV. Assuming that the additive effect observed for the RCs for *Rb. sphaeroides* (Mattioli *et al*., 1995; Allen & Williams, 1995) is valid for other species and the proposed structure for the RC from *C. tepidum* presented here, we would predict a modest increase of the redox potential of about 25 mV as in the case of the FY(M197) mutant and not of *ca*. 100 mV as in the case of the FH(M197) mutant.

The $P^{\circ}/P^{\bullet+}$ redox midpoint potential of isolated RCs from *C. tepidum*, for samples devoid of the cytochrome tetraheme subunit, is +526 mV. Thus, consistent with our predicted effect of the tyrosine residue forming a second H-bond on the P_M C_2 acetyl carbonyl (see above), we observed a *ca.* 25-mV increase of the $P^{\circ}/P^{\bullet+}$ redox midpoint potential in *C. tepidum* RC as compared to that of *Rb. sphaeroides* RC (+500 mV). Moreover, the fact that this extra H-bond does not drastically elevate the redox midpoint potential of the primary donor strongly supports the idea that His L168 (in *Rb. sphaeroides*) largely maintains the redox potential at *ca.* +500 mV. For the primary donor of *Cf. aurantiacus*, the dramatic difference in $P^{\circ}/P^{\bullet+}$ redox midpoint potential compare originates mainly from the absence of His L168 donating a H-bond to the acetyl carbonyl of P_L and not the tyrosine-donated H-bond on the P_M C_2 acetyl carbonyl group (Ivancich *et al.*, 1996).

The $P^{\circ}/P^{\bullet+}$ redox midpoint potential in isolated RCs of *C. tepidum* containing the tetraheme cytochrome *c* subunit (+497 mV) is the same as that observed for chromatophores (+502 mV), within the experimental error. Interestingly, the $P^{\circ}/P^{\bullet+}$ redox midpoint potential in isolated RCs of *C. tepidum* containing the tetraheme cytochrome *c* subunit is *ca.* 20 mV lower than that of RCs devoid of the cytochrome. On the basis of our FT (pre)resonance Raman results, this difference in redox potential cannot be attributed to changes in the H-bonding strengths. For *Rb. sphaeroides*, the $P^{\circ}/P^{\bullet+}$ redox midpoint potential in isolated RCs is *ca.* +500 mV (Lin *et al.*, 1994; Beekman *et al.*, 1995). However, the $P^{\circ}/P^{\bullet+}$ redox midpoint potential in *Rb. sphaeroides* chromatophores appears to be variable, ranging from +440 mV (Dutton & Jackson, 1972) to +465 mV (Drepper, unpublished results measured under similar conditions as for *C. tepidum* chromatophores) to +488 mV (Beekman *et al.*, 1995). This variation, at least for the case of *Rb. sphaeroides*, indicates that several factors in the native membrane also play a role in the fine-tuning of the $P^{\circ}/P^{\bullet+}$ redox midpoint potential. Nevertheless, it is clear that no matter how one compares them, the oxidation potential of P in *C. tepidum* is higher than that of *Rb. sphaeroides* by an amount of *ca.* +25 mV (but much less than +100 mV) as predicted (see above).

The thermostability of the antenna and reaction center membrane proteins of the photosynthetic apparatus of thermophilic *C. tepidum* was largely attributed to the native membrane (Nozawa *et al.*, 1987). At present there are no clear indications of specific intrinsic features of the *C. tepidum* RC protein which could be ascribed as contributing to its thermal stability. The primary structure is similar to those of mesophilic photosynthetic purple bacteria such as *Rb. sphaeroides*, *Rps. viridis*, and *Rb. capsulatus*. The amino acid residues (i.e., His L176, and Tyr M196) donating H-bonds to the conjugated carbonyl groups of P are also not unusual for other mesophilic species such as *Rps. viridis*. However, as gauged by FT Raman vibrational investigations, RCs of *C. tepidum*, like those of thermophilic *Cf. aurantiacus* (Ivancich *et al.*, 1996), show less temperature-dependent conformational changes at the level of the C_9 keto carbonyl of P_L than that of mesophilic *Rb. sphaeroides*, reflecting that the former two RCs are more inflexible or rigid. It is generally believed that the thermal stability of a protein increases as its conformational flexibility is reduced (Cowan, 1995).

CONCLUSION

We have characterized the primary donor of the purple sulfur bacterium, *C. tepidum* by near-infrared FT (pre)-resonance Raman spectroscopy and the partial sequence alignment of the L and M protein subunits with those from *Rb. sphaeroides* and *Rps. viridis*, in the vicinity of the primary donor. From our deduced structural model, the primary donor of *C. tepidum* is constituted of two BChl *a* molecules, each of them possessing a sole axial ligand donated by histidine residues (His L181 and His M201). Interestingly, both C_2 acetyl carbonyl groups are H-bonded while both C_9 keto carbonyls are free from interactions with the protein; this H-bond pattern is different to that of *Rb. sphaeroides* primary donor for which an asymmetric protein interaction is observed; i.e., only the P_L C_2 acetyl carbonyl is H-bonded to His L168 (El-Kabbani *et al.*, 1991; Chirino *et al.*, 1994; Ermler *et al.*, 1994). In the primary donor of *C. tepidum*, the P_L C_2 acetyl carbonyl is also H-bonded to a His residue (His L176) while that on the M side is H-bonded to a Tyr residue (Tyr M196). The H-bond on the L side is stronger than that of *Rb. sphaeroides*. The extra tyrosine-donated H-bond on the acetyl carbonyl of P_M modestly raises (by 25 mV) the $P^{\circ}/P^{\bullet+}$ redox midpoint potential of *C. tepidum* RCs without tetraheme cytochrome subunit (+526 mV) as compared to that of *Rb. sphaeroides* RCs (+500 mV), which strongly supports the fact that it is His L168 which maintains the redox potential at *ca.* +500 mV. The positive charge is more delocalized over both BChl molecules (estimated 69% localization on P_L) as compared to the primary donor of *Rb. sphaeroides* (estimated 80% localization on P_L).

ACKNOWLEDGMENT

We thank Drs. M. Lutz and P. Mathis for their support of this work.

REFERENCES

Agalidis, I., Robert, B., Mattioli, T. A., & Reiss-Husson, F. (1992) in *The Photosynthetic Bacterial Reaction Center II* (Breton, J., & Verméglio, A., Eds.), pp 133−139, Plenum Press, New York.

Allen, J. P., & Williams, J. C. (1995) *J. Bioenerg. Biomembr. 27*, 275−283.

Beekman, L. M. P., Visschers, R. W., Monshouwer, R., Heer-Dawson, M., Mattioli, T. A., McGlynn, P., Hunter, C. N., Robert, B., van Stokkum, I. H. M., van Grondelle, R., & Jones, M. R. (1995) *Biochemistry 34*, 14712−14721.

Blankenship, R. E. (1992) *Photosynth. Res. 33*, 91−111.

Bruce, B. D., Fuller, R. C., & Blankenship, R. E. (1982) *Proc. Natl. Acad. Sci. U.S.A. 79*, 6532−6536.

Chirino, A. J., Lous, E. J., Huber, M., Allen, J. P., Schenck, C. C., Paddock, M. L., Feher, G., & Rees, D. C. (1994) *Biochemistry 33*, 4584−4593.

Clark, W. M. (1960) *Oxidation−Reduction Potentials of Organic Systems*, Williams and Wilkins, Baltimore, MD.

Cotton, T. M., & Van Duyne (1981) *J. Am. Chem. Soc. 103*, 6020−6026.

Cowan, D. A. (1995) in *Essays in Biochemistry* (Apps, D. K., & Tipton, K. F., Eds.) Vol. 29, pp 193−206, Portland Press, London.

Deisenhofer, J., & Michel, H. (1989) *EMBO J. 8*, 47−54.

Deisenhofer, J., Epp., O., Sinning, I., & Michel, H. (1995) *J. Mol. Biol. 246*, 429−457.

Donohoe, R. J., Duchowski, J. K., & Bocian, D. F. (1988) *J. Am. Chem. Soc. 110*, 6119−6124.

Duchowski, J. K. & Bocian, D. F. (1990) *J. Am. Chem. Soc. 112*, 8807−8811.

Dutton, P. L., & Jackson, J. B. (1972) *Eur. J. Biochem. 30*, 495−510.

Dutton, P. L., & Wilson, D. F. (1974) *Biochim. Biophys. Acta 346*, 165−212.
Ermler, U., Fritzsch, G., Buchanan, S. K., & Michel, H. (1994) *Structure 10*, 925−936.
Feiler, U., Albouy, D., Robert, B., & Mattioli, T. A. (1995) *Biochemistry 34*, 1099−1105.
Garcia, D., Parot, P., Verméglio, A., & Madigan, M. T. (1986) *Biochim. Biophys. Acta 850*, 390−395.
Garcia, D., Parot, P., & Verméglio, A. (1987) *Biochim. Biophys. Acta 894*, 379−385.
Goldsmith, J. O., King, B., & Boxer, S. G. (1996) *Biochemistry 35*, 2421−2428.
Heald, R. L., & Cotton, T. M. (1990) *J. Phys. Chem. 94*, 3968−3975.
Ivancich, A., Feick, R., Ertlmaier, A., & Mattioli, T. A. (1996) *Biochemistry 35*, 6126−6135.
Katayama, N., Kobayashi, M., Motojima, F., Inaka, F., Nozawa, T., & Miki, K. (1994) *FEBS Lett. 348*, 158−160.
Kobayashi, M., & Nozawa, T. (1993) *Bull. Chem. Soc. Jpn. 66*, 3834−3836.
Kobayashi, M., Wang, Z.-Y., Yoza, K., Umetsu, M., Konami, H., Mimuro, M., & Nozawa, T. (1996) *Spectrochim. Acta 51A*, 585−589.
Koyama, Y., Umemoto, Y., Akamatsu, A., Uehara, K., & Tanaka, M. (1986) *J. Mol. Struct. 146*, 273−287.
Krawczyk, S. (1989) *Biochim. Biophys. Acta 976*, 140−149.
Lin, X., Murchison, H. A., Nagarajan, V., Parson, W. W., Williams, J. C., & Allen, J. P. (1994) *Proc. Natl. Acad. Sci. U.S.A. 91*, 10265−10269.
Lutz, M. (1984) in *Advances in Infrared and Raman Spectroscopy* (Clark, R. J. H., & Hester, R. E., Eds.) Vol. 11, pp 211−300, Wiley, New York.
Lutz, M., & Robert, B. (1988) in *Biological Applications of Raman Spectroscopy* (Spiro, T. G., Ed.) Vol. 3, pp 347−411, John Wiley & Sons, New York.
Madigan, M. T. (1984) *Science 225*, 313−315.
Madigan, M. T. (1986) *Int. J. Syst. Bacteriol. 36*, 222−227.
Mäntele, W. G., Wollenwebber, A. M., Nabedryk, E., & Breton, J. (1988) *Proc. Natl. Acad. Sci. U.S.A. 85*, 8468−8472.
Mattioli, T. A., Hoffmann, A., Robert, B., Schrader, B., & Lutz, M. (1991) *Biochemistry 30*, 4648−4654.
Mattioli, T. A., Robert, B., & Lutz, M. (1992a) in *The Photosynthetic Bacterial Reaction Center II* (Breton, J., & Verméglio, A., Eds.) pp 127−132, Plenum Press, New York.
Mattioli, T. A., Sockalingum, D., Lutz, M., & Robert, B. (1992b) in *Research in Photosynthesis* (Murata, N., Ed.) Vol. I, pp 405−408, Kluwer, Dordrecht, The Netherlands.
Mattioli, T. A., Hoffmann, A., Sockalingum, D. G., Schrader, B., Robert, B., & Lutz, M. (1993) *Spectrochim. Acta 49A*, 785−799.
Mattioli, T. A., Williams, J. C., Allen, J. P., & Robert, B. (1994) *Biochemistry 33*, 1636−1643.
Mattioli, T. A., Lin, X., Allen, J. P., & Williams, J. C. (1995) *Biochemistry 34*, 6142−6152.
Michel, H., Weyer, K. A., Gruenberg, H., Dunger, I., Oesterhelt, D., & Lottspeich, F. (1986) *EMBO J. 5*, 1149−1158.
Moss, D. A., Leonhard, M., Bauscher, M., & Mäntele, W. (1991) *FEBS Lett. 283*, 33−36.
Nagashima, K. V. P., Shimada, K., & Matsuura, K. (1993) *Photosynth. Res. 36*, 185−191.
Nagashima, K. V. P., Matsuura, K., Ohyama, S., & Shimada, K. (1994) *J. Biol. Chem. 269*, 2477−2484.
Nozawa, T., & Madigan, M. T. (1991) *J. Biochem. (Tokyo) 110*, 588−594.
Nozawa, T., Fukada, T., Hatano, M., & Madigan, M. T. (1986) *Biochim. Biophys. Acta 852*, 191−197.
Nozawa, T., Trost, J. T., Fukada, T., Hatano, M., McManus, J. D., & Blankenship, R. E. (1987) *Biochim. Biophys. Acta 894*, 468−476.
Palaniappan, V., & Bocian, D. F. (1995) *J. Am. Chem. Soc. 117*, 3647−3648.
Palaniappan, V., Aldema, M. A., Frank, H. A., & Bocian, D. F. (1992) *Biochemistry 31*, 11050−11058.
Palaniappan, V., Martin, P. C., Chynwat, V., Frank, H. A., & Bocian, D. F. (1993) *J. Am. Chem. Soc. 115*, 12035−12049.
Robert, B. (1990) *Biochim. Biophys. Acta 1017*, 99−111.
Robert, B., & Lutz, M. (1988) *Biochemistry 27*, 5108−5114.
Romijin, J. C., & Amesz, J. (1977) *Biochim. Biophys. Acta 461*, 327−338.
Shiozawa, J. A., Lottspeich, F., Oesterhelt, D., & Feick, R. (1989) *Eur. J. Biochem. 180*, 75−84.
Shreve, A. P., Cherepy, N. J., Franzen, S., Boxer, S. G., & Mathies, R. A. (1991) *Proc. Natl. Acad. Sci. U.S.A. 88*, 11207−11211.
Tran-Thi, T.-H., Mattioli, T. A., Chabach, D., de Cian, A., & Weiss, R. (1994) *J. Phys. Chem. 98*, 8279−8288.
Venturoli, G., Mallardi, A., & Mathis, P. (1993) *Biochemistry 32*, 13245−13253.
Wachtveitl, J., Farchaus, J. W., Das, R., Lutz, M., Robert, B., & Mattioli, T. A. (1993) *Biochemistry 32*, 12875−12886.
Williams, J. C., Steiner, L. A., Ogden, R. C., Simon, M. I., & Feher, G. (1983) *Proc. Natl. Acad. Sci. U.S.A. 80*, 6505−6509.
Williams, J. C., Steiner, L. A., Feher, G., & Simon, M. I. (1984) *Proc. Natl. Acad. Sci. U.S.A. 81*, 7303−7307.
Williams, J. C., Alden, R. G., Murchison, H. A., Peloquin, J. M., Woodbury, N. W., & Allen, J. P. (1992) *Biochemistry 31*, 11029−11037.
Woese, C. R. (1987) *Miocrobiol. Rev. 51*, 221−271.
Yeates, Y. O., Komiya, H., Chirino, A., Rees, D. C., Allen, J., & Feher, G. (1988) *Proc. Natl. Acad. Sci. U.S.A. 85*, 7993−7997.

BI953047J